BULETINUL INSTITUTULUI POLITEHNIC DIN IAŞI
Publicat de
Universitatea Tehnică „Gheorghe Asachi” din Iaşi
Volumul 70 (74), Numărul 4, 2024
Secţia
CONSTRUCŢII DE MAŞINI
DOI:10.2478/bipcm-2024-0021

STUDY OF THE CHARACTERISTICS OF GFRP COMPOSITE MATERIALS, APPLIED IN MECHANICAL ENGINEERING

BY

NICOLETA IFTIMIE[1,2], CIPRIAN-IONUȚ MORĂRAŞ[1,*], VIOREL GOANȚĂ[1] and PAUL-DORU BÂRSĂNESCU[1]

[1]“Gheorghe Asachi” Technical University of Iași,
Faculty of Mechanical Engineering
[2]Nondestructive Testing Department, National Institute of Research and Development for Technical Physics, Iași

Received: January 30, 2025
Accepted for publication: February 11, 2025

Abstract. Glass fiber reinforced (GFRP) polymer composites have been prepared by various manufacturing technologies and are widely used for various applications. Fiber glass composites possess good properties such as high strength, flexibility, rigidity, durability, etc. Compared to composite materials reinforced with unidirectional distributed fibers, composites reinforced with fabric have the advantage of the balance achieved between the mechanical and elastic properties in the 0° and 90° directions, although in one of the directions the modulus of elasticity and tensile strength are lower, due to the presence of fiber undulations when reinforcing with fabrics. In this work, a comparison is made between the elastic characteristics of GFRP, determined by tension and by 4 - point bending test.

Keywords: GFRP materials, defects, strain-stress, tensile, flexure.

---

[*]Corresponding author; *e-mail*: ciprian-ionut.moraras@academic.tuiasi.ro

1. Introduction

Defects appear in composite materials at the interlaminar level and evolve under the action of the stresses to which the structures are subjected during operation. Thus, a defect caused by an impact at low speed may initially not be visible to the naked eye, as later during exploitation, due to fatigue, it becomes visible even through a catastrophic effect. Over the years, there have been events with consequences and causes that have aroused a special interest among researchers in the study of the causes and evolution of defects in composite materials used in mechanical engineering.

The behaviour and material properties of unidirectional glass fiber reinforced composites under static and low temperature conditions were studied (Torabizadeh, 2013). Tensile, compression and shear tests were performed at low temperatures and it was found that as the temperature decreased the tensile strength and Young's modulus of the laminates increased until breaking.

Studies were also made on the effect of fiber loading, tensile orientation and impact resistance of composite polymer materials (Adekomaya and Adama, 2017). The main key of this research study is that it defines the properties of composites through fiber loading and direction. The strength and stiffness properties are also increased by the volume percentage of fiber in GFRP composites. The nature of fatigue in GFRP composites under combined torsional and bending loading at room temperature was investigated (El-Assal and Khashaba, 2007). A series of torsional fatigue tests were conducted to establish the failure pattern of the GFRP composite using different failure theories. The results showed that unidirectional glass fiber reinforced polyester composites have low torsional fatigue strength compared to the experimental results on flexural fatigue strength. Wind turbine blades are often made of GFRP due to the combination of light weight and mechanical strength, which allows the design of large and efficient turbines (Iftimie *et al*., 2018; Savin *et al*., 2018). The paper presents the experimental results in tensile and flexural testing on GFRP composite material reinforced in two normal directions.

2. Material and methods

The orthotropic composite material is characterized by three elastic characteristics corresponding to each orthogonal plane, the elastic moduli E_{11}, E_{22}, E_{33}, the shear moduli G_{12}, G_{13}, G_{23} and the Poisson coefficients ν_{12}, ν_{13}, ν_{23} (Ranković *et al*., 2010). The indices define the direction of the elastic characteristic, the first index the loading direction and the second representing the direction in which the elastic characteristic is determined (Mallick, 2007). Thus, for the calculation of the Poisson's ratio in the plane in the two directions, we define:

$$\nu_{12} = \left| \frac{\varepsilon \text{ on direction } 2}{\varepsilon \text{ on loading direction } 1} \right|$$
$$\nu_{21} = \left| \frac{\varepsilon \text{ on direction } 1}{\varepsilon \text{ on loading direction } 2} \right| \tag{1}$$

Similarly, specific stresses and strains are also noted with two indices: the first represents the direction normal to the plane on which the stress or strain load and the second denote the direction to which it is parallel (Mian *et al.*, 2007). In Fig. 1 is represented schematically of the three planes of symmetry and the main directions of an orthotropic material.

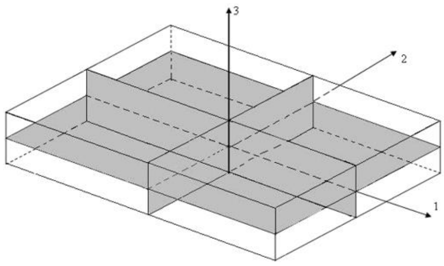

Fig. 1 – Symmetry planes of orthotropic material.

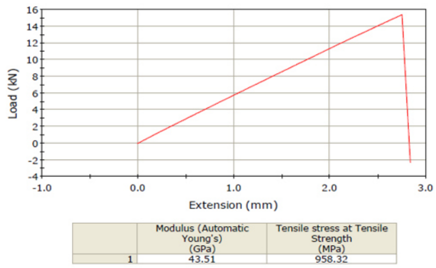

Fig. 2 – C-epoxy load – extension diagram.

The specimen from MC, with beads to strengthen the clamping areas in the tanks (ASTM D3039) has w = 12.7 mm for the specimen reinforced only in the direction of tensile test (0°) and w = 25.4 mm for the one reinforced in the direction normal to the direction of tensile test (90°) or at ± 45°; t = 0.5÷2.5 mm.

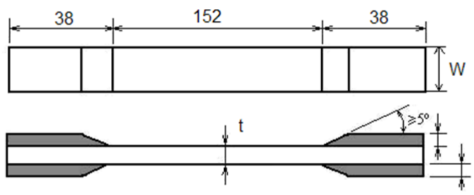

Fig. 3 – The specimen taken in the study.

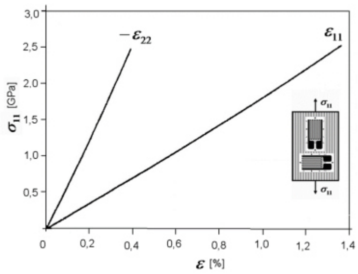

Fig. 4 – Stress - strain curve for specimen [0_6] (longitudinally reinforced).

The specimen has T-type rosettes glued on both sides (to detect if there is possible bending), oriented according to the main directions of the material. In this case, the directions of main stresses and deformations coincide.

Cutting the specimens from a GFRP composite plate, 4mm thick, reinforced with 10 layers of glass fiber at [0°/90°]. The sampling method of the samples was along the longitudinal, transversal and 45° directions, as in Fig. 5. The dimensions of the samples are: 145x 25.4x4mm and 145x12.7x4mm respectively. The tensile stress of the composite specimen was fixed in the grips of the universal testing machine (type INSTRON 8801) to determine the material characteristics complying with the provisions of the ASTM D 3039 standard.

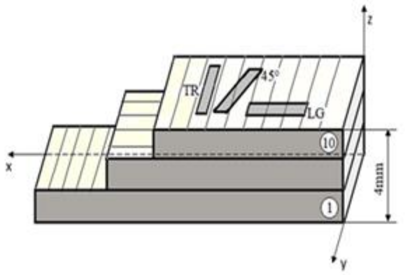

(a)

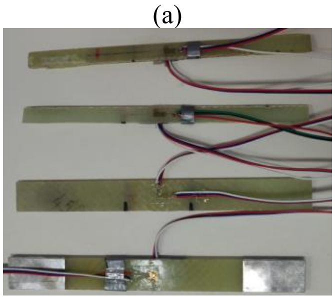

(b)

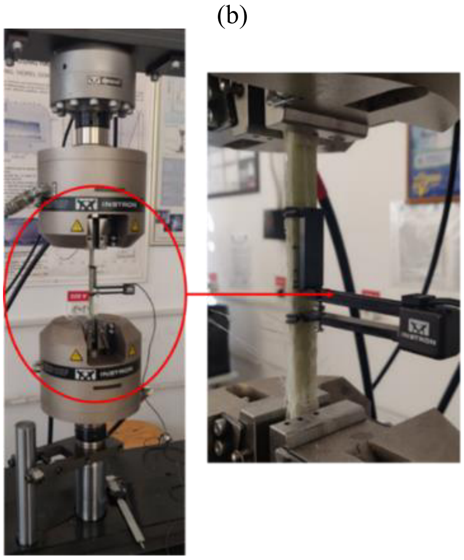

(c)

Fig. 5 – (a) Sampling directions of the GFRP specimen; (b) Specimens for tensile and bending test; (c) Tensile test and details with extensometer positioning on specimen (INSTRON 8801 testing machine).

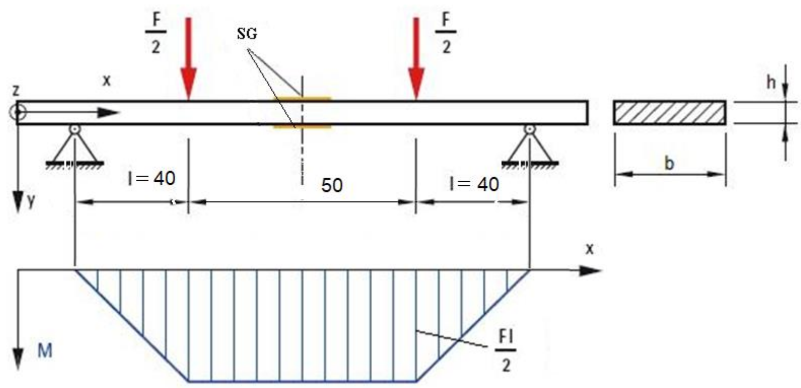

Fig. 6 – Specimen can be placed with the T rosette above or below.

To measure the shear modulus of elasticity G_{12}, samples are cut after the bisector of the right angle 1O2. Using the T^{ε} matrix for the 45° rotation around axis 3, we get:

$$G_{xy} = \frac{\sigma_{xx}}{2(\varepsilon_{xx} - \varepsilon_{yy})} \tag{2}$$

For this specimen the slips γ are not zero. Loading was done at a speed of 2mm/min, with displacement control, on three samples, loaded at 0°, 90° and 45°. Two strain gauges were glued on each specimen, in the longitudinal and transverse direction. After completing the test, it is desired to draw the diagrams in the Figs. 8-12.

Fig. 7 – The experimental device for 4-point bending on the INSTRON 34SC-5 testing machine.

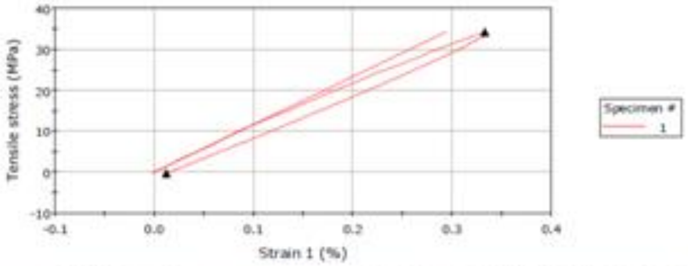

	Tensile extension at Yield (Zero Slope) (mm)	Modulus (Automatic) (MPa)	Tensile stress at Tensile Strength (MPa)	Tensile strain at Tensile Strength (mm/mm)
1	-----	11631.49628	34.27985	0.00332

	Load at Tensile Strength (N)	Tensile extension at Tensile Strength (mm)	Tensile stress at Break (Standard) (MPa)	Tensile strain at Break (Standard) (mm/mm)
1	3495.50247	0.16623	-0.03455	0.00012

	Load at Break (Standard) (N)	Tensile extension at Break (Standard) (mm)	Energy at Break (Standard) (J)	Geometry
1	-3.52263	0.00613	0.04618	Rectangular

Fig. 8 – Stress-strain diagram, provided by the testing machine, for a loading-unloading cycle.

3. Determination of the elastic characteristics of GFRP by the tensile test

A specimen test at 45°, on which a "T" type strain gauge was glued, was tested for tensile test, in order to determine the Young's modulus of elasticity and the Poisson's ratio. Figure 9 shows the stress-strain diagram (indicated by the testing machine - the specific elongation (indicated by the longitudinal strain gauge SG), which results in E = 10852 MPa, and Fig. 10 shows the stress–strain diagram (strain indicated by the transversal SG). Figure 11 shows the longitudinal strain - transversal strain, from which the Poisson coefficient ν = 0.695 results.

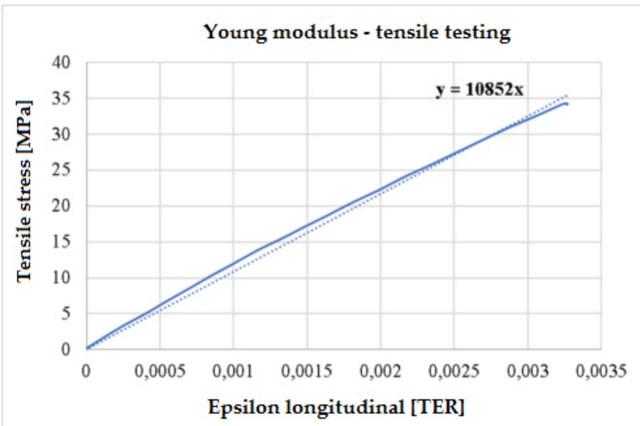

Fig. 9 – Stress – strain diagram (strain indicated by longitudinal SG).

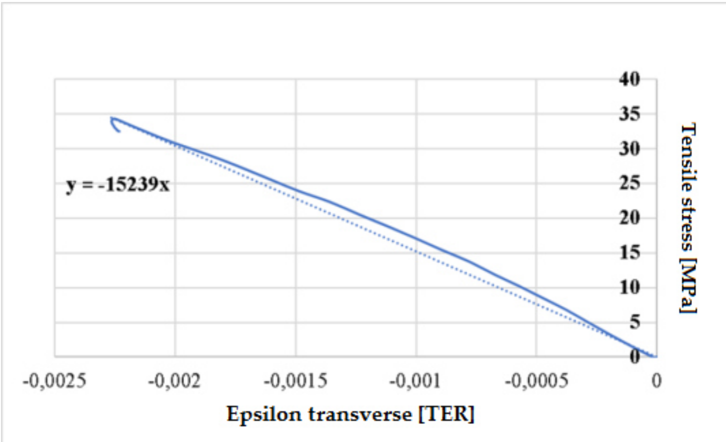

Fig. 10 – Stress – strain diagram (strain indicated by transversal SG).

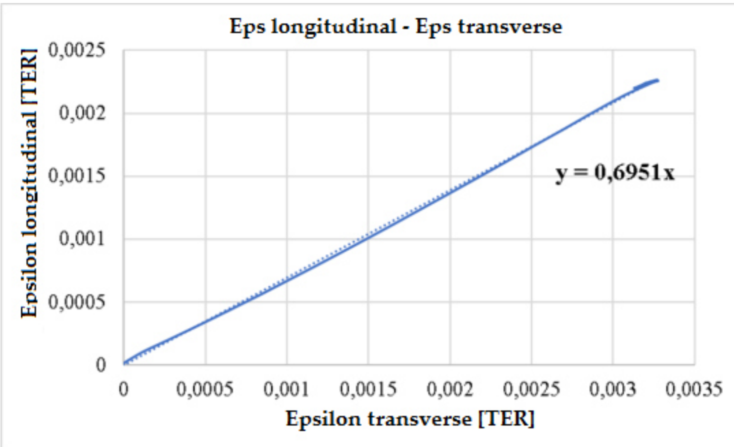

Fig. 11 – Diagram longitudinal strain - transversal strain.

4. Determination of elastic characteristics of GFRP by four-point bending

Figures 12-16 show the test results of the specimen test at 45° for a loading-unloading cycle. In Fig. 13 it is represented the variation of the output signals from the two strain gauges vs. time and in Fig. 14 diagram stress (at the surface of the specimen) – strain (given by the strain gauge mounted longitudinally), E = 22004 MPa. In Fig. 15 is represented the transverse strain as a function of longitudinal strain (both provided by strain gauges), Poisson's ratio ν = 0.497 and in Fig. 16 diagram stress (on the surface of the specimen) as a function of $2(\varepsilon_{long}-\varepsilon_{transv})$, the transverse modulus of elasticity G=7333.5 MPa (see relation 2).

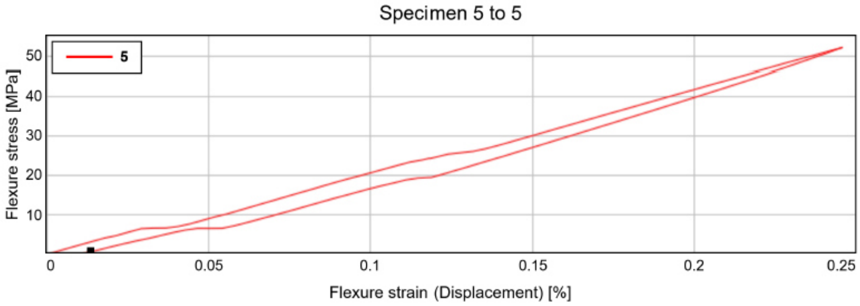

	Displacement at Break (Standard) [mm]	Energy at Break (Standard) [J]	Flexure displacement at Break (Standard) [mm]
5	0.12	0.01	0.12

	Flexure strain (Displacement) at Break (Standard) [%]	Flexure stress at Break (Standard) [MPa]	Force at Break (Standard) [kN]
5	0.01	0.78	0.00

	Status number at Break (Standard)	Time at Break (Standard) [s]
5	1	128.97

Fig. 12 – Flexure stress (at the surface of the specimen) vs. flexure strain diagram provided by the testing machine.

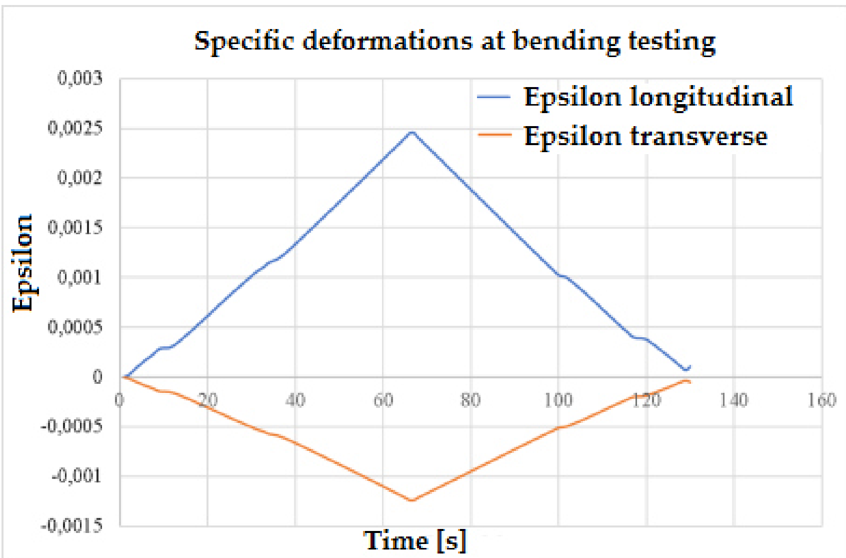

Fig. 13 – Variation of the output signals from the two strain gauges vs. time.

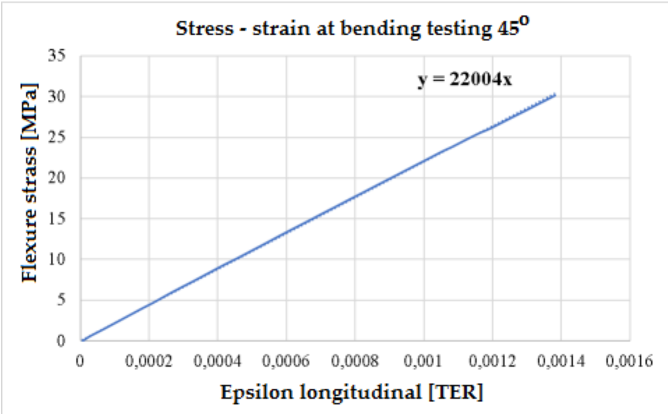

Fig. 14 – Stress-strain diagram.

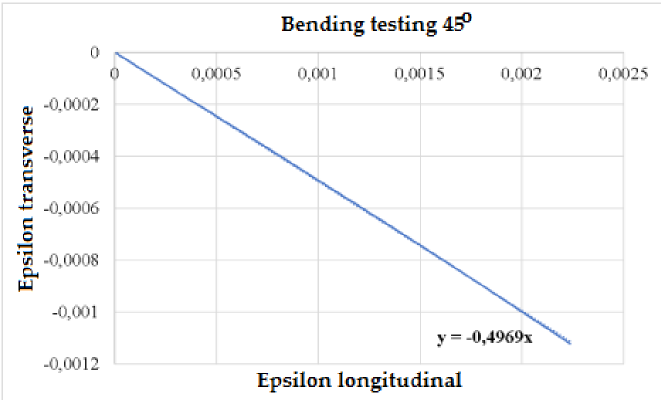

Fig. 15 – The transverse strain vs. longitudinal strain.

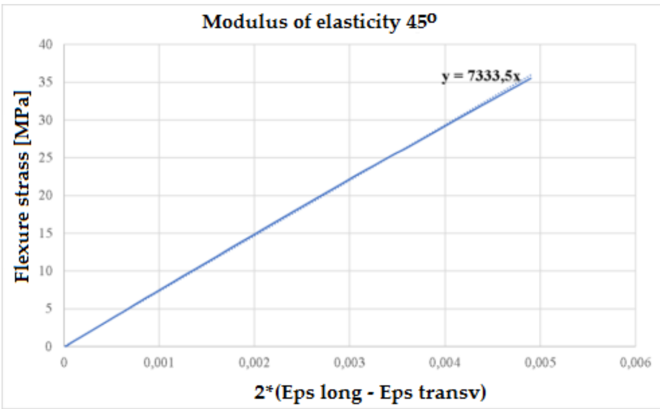

Fig. 16 – Diagram stress vs. $2(\varepsilon_{long}-\varepsilon_{transv})$.

5. Conclusions

Some elastic characteristics of GFRP composite material reinforced in two normal directions were determined by tensile and bending testing, respectively. For this purpose, specimens were cut from the GFRP plate along the 0°, 90° and 45° directions. In this paper, the results for the sample cut along the 45° direction are presented, and in another paper we will also present the results for the samples cut at 0° and 90°. Strain gauges type "T" were glued on all the samples. The specimens at 45° were tested at tension and bending, the experimental data were acquired and processed. The values of the elastic characteristics determined are comparable to those obtained by other authors (Moraras *et al.*, 2023), except for the Poisson's ratio obtained by traction and the Young's modulus obtained by bending, both with specimens at 45°. The tests performed showed, in general, similar values of the characteristics determined in tensile and flexure testing, with few exceptions, which are to be investigated later. In the case of bending the specimens at 45°, torsion may also occur, and special supports are required to prevent this.

Acknowledgements. This work was supported by Romanian Ministry of Education and Research, Program Nucleu PN 23 11 01 02.

REFERENCES

Adekomaya O., Adama K., *Glass-fiber reinforced composites: The effect of fiber loading and orientation on tensile and impact strength*, Nigerian J. Technol. 36 (3), pp. 782-787 (2017).

El-Assal A., Khashaba U., *Fatigue analysis of unidirectional GFRP composites under combined bending and torsional loads*, Comp. Struct. 79 (4), pp. 599-605 (2007).

Iftimie N., Steigmann R., Dobrescu G.S., Danila N.A., Savin A., Barsanescu P.D., Goanta V., *Scalable Wind Turbine Blades nondestructive evaluation using different types of sensors*, In IOP Conference Series: Materials Science and Engineering, vol. 444(2), p. 022006, 2018, IOP Publishing1757-8981.

Mallick P.K., *Fiber Reinforced Composites Materials*, 3rd Ed., 2007.

Mian A., Han X., Islam S., Newaz G., *Fatigue damage detection in graphite/epoxy composites using sonic infrared imaging technique*, Composites Science and Technology 64, 2004, pp. 657-666.

Morăras C.I., Goantă V., Husaru D., Istrate B., Barsanescu P.D., Munteanu C., *Analysis of the Effect of Fiber Orientation on Mechanical and Elastic Characteristics at Axial Stresses of GFRP Used in Wind Turbine Blades*, Polymers 2023, 15(4), 861.

Ranković S., Folić R., Mijalković M., *Effects of RC beams reinforcement using near surface mounted reinforced FRP composites*, Series: Architecture and Civil Engineering, Vol. 8(2), 177-185 (2010).

Savin A., Iftimie N., Steigmann R., Rosu D., Dobrescu et al., *Effective methods for Structural Health Monitoring of critical zones of scalable wind turbine blades*, Strojniski Vestnik/J. of Mech. Eng., 64(11), pp. 680-689 (2018).

Torabizadeh M.A., *Tensile, compressive and shear properties of unidirectional glass/epoxy composites subjected to mechanical loading and low temperature services*, 2013.

STUDIUL CARACTERISTICILOR MATERIALELOR COMPOZITE GFRP, APLICATE ÎN INGINERIA MECANICĂ

(Rezumat)

Compozitele armate cu fibra de sticlă (GFRP) posedă proprietăți bune precum rezistență ridicată, flexibilitate, rigiditate, durabilitate, cost redus etc. În comparație cu materialele compozite armate cu fibre distribuite unidirecționale, compozitele armate cu țesătură au avantajul echilibrului realizat între proprietățile mecanice și elastice pe direcțiile 0° și 90°, deși într-una dintre direcții modulul de elasticitate și rezistența la tracțiune sunt puțin mai mici, datorită prezenței ondulațiilor fibrelor la armarea cu țesături. În această lucrare se face o comparație între caracteristicile elastice ale GFRP, determinate prin încercări de tracțiune și încovoiere în patru puncte.